

Effect of citric acid and plasma activated water on the functional properties of sodium alginate for potential food packaging applications

Nusrat Sharmin^{a,*}, Izumi Sone^a, James Leon Walsh^b, Morten Sivertsvik^a, Estefanía Noriega Fernández^a

^a Department of Processing Technology, Nofima AS, Richard Johnsen's Gate 4, 4021, Stavanger, Norway

^b Centre for Plasma Microbiology, Department of Electrical Engineering & Electronics, University of Liverpool, Liverpool, L69 3BX, UK

ARTICLE INFO

Keywords:

Sodium alginate
Plasma activated water (PAW)
Citric acid
Cross-linking

ABSTRACT

In this study, cold plasma activated water (PAW) was used in the preparation of sodium alginate (SA) solution and the effect of reactive oxygen and nitrogen species (RONS), low pH and high oxidation-reduction potential on the functional properties of SA films was evaluated. Citric acid (CA) was added to SA, and the combined effect of PAW and CA on the functional properties of SA films was assessed. With 0.5, 1 and 2 w/v% addition of CA, tensile strength (TS) of the SA films decreased by 32, 58 and 66 %, while the elongation at break (EB) increased by 150, 275 and 475 %. The TS and EB of SA films increased by 43 and 66 % when PAW was used to prepare SA solutions. Addition of glycerol reduced the TS and tensile modulus, while the EB was increased. The linear viscoelastic region (LVE) of SA decreased with the addition of CA and glycerol. However, addition of PAW increased the LVE region. The 1 and 2 % CA and PAW containing samples showed higher storage modulus as compared to the control samples and no intersection was observed between storage and loss modulus. The CA and/or PAW containing solutions showed shear thinning properties. The water vapour transmission rate (WVTR) of SA decreased by 34 % with the addition of 1 % CA, while only 12 % reduction was observed for 0.5 and 2 % CA containing samples. A further reduction in WVTR to 44 % was observed as PAW was added to 1 % CA containing SA samples.

1. Introduction

In recent years, much awareness has been made on the development of biodegradable films for food packaging based on materials from renewable sources. Commonly investigated materials for food packaging are polysaccharides, proteins, and lipids (Carissimi, Flôres, & Rech, 2018; Cazón, Velazquez, Ramírez, & Vázquez, 2017; Qin, Mo, Liao, He, & Sun, 2019). Among these, polysaccharides based materials (e.g., alginate) have attracted attention due to low cost, excellent film forming capacity and abundant resources (Carissimi et al., 2018). SA is a non-toxic and biocompatible natural linear block copolymer which is composed of β -D-mannuronic and α -L-guluronic acid residues linked by a β -(1-4) glycosidic bond (Nasrollahzadeh, Sajjadi, Irvani, & Varma, 2021). Films made from alginate generally have good tensile strength, flexibility and O₂ barrier properties which is beneficial for potential food packaging applications (Shahabi-Ghahfarrokhi, Almasi, & Babaei-Ghazvini, 2020). Another benefit of using alginate as for food

packaging is the organoleptic properties of alginates, being relatively taste and odourless (Puscaselu, Gutt, & Amariei, 2019). The great interest for SA is also inextricably associated to its gelling properties. SA can form gels either by lowering the pH below the pK_a value of the uronic residue or in presence of divalent cations (Russo, Malinconico, & Santagata, 2007). The divalent ions cooperatively interact with blocks of guluronic units to form ionic bridges between different chains. The ability to form this kind of interaction is strongly influenced by the length, distribution and the ratio of different blocks (Lee & Mooney, 2012).

SA is a pH sensitive polymer and the pH sensitivity of SA is mainly due to the presence of a large number of $-\text{COO}^-$ reactive groups in the structure and thus, the formation of alginate gels can be induced via acidic cross-linking (Hua, Ma, Li, Yang, & Wang, 2010). Under acidic conditions the $-\text{COO}^-$ is converted to COOH enhancing hydrogen bond interaction between the carboxyl groups of alginate chains. Such interaction can significantly alter the mechanical, rheological and barrier

* Corresponding author.

E-mail address: Nusrat.sharmin@nofima.no (N. Sharmin).

<https://doi.org/10.1016/j.fpsl.2021.100733>

Received 13 March 2021; Received in revised form 14 July 2021; Accepted 19 July 2021

Available online 26 July 2021

2214-2894/© 2021 The Author(s). Published by Elsevier Ltd. This is an open access article under the CC BY license (<http://creativecommons.org/licenses/by/4.0/>).

properties of sodium alginate due to the shrinkage of the molecular chain (Zou et al., 2020). On the contrary, when the pH increases, the $-COOH$ group ionizes to $-COO^-$, which can increase the hydrophilicity of the sodium alginate due to the extension of the molecular chain (Zou et al., 2020). Moreover, the viscosity of SA is a very important factor governing the gel homogeneity which can be modified by adjusting the pH of the solution (Tavassoli-Kafrani, Shekarchizadeh, & Masoudpour-Behabadi, 2016). A uniform viscosity of the solution is very important for achieving a uniform film thickness which can eventually affect the mechanical properties.

Cross-linking is a promising technique to improve the functional properties of polysaccharide films. Several cross-linking agents like glutaraldehyde, boric acid etc. have been used to cross link polysaccharides films (Fan, Duquette, Dumont, & Simpson, 2018; Khan et al., 2018). However, the selection of cross-linking agents becomes limited in the context of food packaging applications due to their toxicity and relatively high cost. Citric acid (CA) is a biobased polycarboxylic acid extracted from citrus fruits, which is a low cost and non-toxic natural acid with the ability to cross-link and stabilize polysaccharide structures (Olsson, Hedenqvist, Johansson, & Järnström, 2013). CA can cross-link the polysaccharide chains creating covalent intermolecular di-ester linkages between the carboxyl groups of the cross-linking agents and hydroxyl groups of the polysaccharide (Azeredo & Waldron, 2016). It is also worth mentioning that SA films could become rigid and brittle after cross linking. Plasticizers such as glycerol can improve the flexibility and processibility of SA by increasing the interchain spacing and reducing interchain interactions (Gao, Pollet, & Avérous, 2017). However, the incorporation of plasticizers in SA solution generally results in a decrease of tensile strength and Young's modulus and an increase of elongation at break of the films (Gao et al., 2017).

Cold plasma (CP), generated at atmospheric pressure and room temperature, consist of ultraviolet photons, electrons, free radicals, positive & negative ions, and excited & non-excited molecules and atoms, which can break covalent bonds and initiate different chemical reactions (Oh, Roh, & Min, 2016). CP is typically induced by the application of an electric discharge in a gas subset (e.g., room air); the partially ionised air assembles a bunch of subatomic/molecular entities (reactive oxygen and nitrogen species, RONS) besides quanta of electromagnetic radiation (UV-photons, visible light). CP treatment has been widely used for surface functionalization, etching, polymer degradation and cross-linking reactions (Nielsen-Nygaard et al., 2021; Pankaj et al., 2014). A recent application of this technology focuses on the activation of liquids such as water through their exposure to CP discharges, e.g. using air as the CP working gas (creating air plasma), resulting in a cocktail of reactive oxygen and nitrogen species (RONS) (Risa Vaka et al., 2019). The type and concentration of reactive species present in the plasma activated water (PAW) can alter the pH of the solution (e.g. acidification) and increase the oxidation and reduction potential (ORP) and conductivity, depending on operating parameters such as the configuration of the CP source, dissipated plasma power, activation time, etc. (Risa Vaka et al., 2019). PAW is classified neither as a chemical reagent nor a natural resource but as purified water, with promising applications in the food industry (Thirumdas et al., 2018). The combined action of RONS, low pH and high ORP has been acknowledged as the main contributor to the observed PAW preservation efficacy.

The main aim of the present study was to evaluate the effect of different concentrations of CA and PAW on the mechanical, rheological and barrier properties of SA. The pH of PAW normally varies between 2–3. Therefore, the concentration of CA was selected to match the final pH level between 2.5–3.5 in order compare the functional properties of the CA containing SA with the functional properties of SA solution prepared with PAW. Finally, the combined effect of CA and PAW on the mechanical, rheological and barrier properties of SA was also evaluated.

2. Materials and methods

2.1. Materials

Sodium alginate (alginic acid sodium salt from brown algae) with guluronic acid content ~65–70% and mannuronic acid content ~5–35%, citric acid 99 % (molecular weight: 192.12 g/mol), sodium hypophosphite monohydrate (molecular weight: 87.98 g/mol; anhydrous basis), glycerin and 96 % ethanol were purchased from Sigma-Aldrich, Norway.

2.2. Production of plasma activated water

The plasma activated water (PAW) was produced using a high voltage cold plasma (CP) source comprised of an electrode unit with powered and ground electrodes and a dielectric barrier, made from a 1 mm thick quartz disc. The electrodes were adhered to the lid of the treatment chamber and arranged to produce a surface barrier discharge (SBD). The treatment chamber (176 × 174 × 48 mm) had a total electrode area of 144 cm². For 100 mL of tap water (pH 8.0 ± 0.1 at 9–11 °C), the gap distance between the liquid surface and the electrode was 44.8 mm (3.2 mm water column). The CP generating source produced a sinusoidal signal at a frequency of 18 kHz. Based on prior studies (Risa Vaka et al., 2019), PAW generation settings, i.e. activation time (30 min) and plasma power, yielding the lowest pH and the highest levels of reactive species, oxidation reduction potential (ORP) and stability during storage, were selected as the most promising conditions for the trials and eventually, industrial implementation. The system operated at atmospheric pressure, with room air as the plasma-inducing gas. A schematic representation of the production process of nitrites (NO₂⁻), nitrates (NO₃⁻) and hydrogen peroxide (H₂O₂) in the PAW is presented in Fig. 1.

2.3. Characterization of PAW composition

The concentration of some reactive oxygen and nitrogen species (RONS) present in the PAW (Table 1) was determined via standard spectrophotometric methods using a Shimadzu UV Mini 1240 UV/Vis Spectrophotometer (Shimadzu, Tokyo, Japan). The Spectroquant® test kit #109713 (Merck, New Jersey, USA), analogous to DIN 38405-9, was used to determine the concentration of nitrates at a wavelength of 340 nm (Risa Vaka et al., 2019). The nitrites levels were determined with the Griess method, at a wavelength of 548 nm (Griess, 1879; Kleinbongard, Rassaf, Dejam, Kerber, & Kelm, 2002). The titanium sulphate colorimetric method was used to determine concentrations of hydrogen peroxide at a wavelength of 407 nm (Eisenberg, 1943). pH and ORP values in the PAW (Mettler Toledo SevenGo Pro pH/ion meter, Mettler Toledo, Oslo, Norway) were also characterised.

2.4. Preparation of alginate films

The SA films were prepared by using a solution casting process. An aqueous solution was prepared with either deionized water (DW) or PAW containing 2% (w/v) SA, 0.50–2% (w/v) CA and 0.25–1% (w/v) sodium hypophosphite monohydrate (SHP). Depending on the composition, required amount CA (0.50 g/1 g/2 g) and SHP (0.25 g/0.50 g/1 g) was added to water or PAW containing 2 g SA and the solution was stirred at 1000 rpm using a magnetic stirrer for 3 h at room temperature. When the SA was completely dissolved, then 30 % (w/w) glycerin was added to the solution followed by further stirring for 30 min at room temperature. The composition of the solutions with associated sample codes used during the study are presented in Table 2. Films were casted by pouring 20 mL of the prepared solution into 90 mm diameter silicone coated polystyrene petri dishes and allowed to dry for 24 h at room temperature.

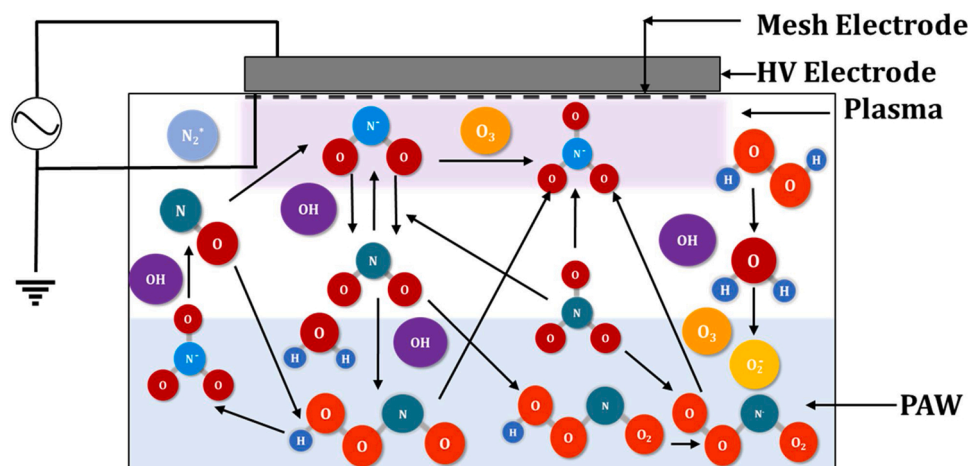


Fig. 1. Schematic representation of the experimental setup for the plasma generation. (Images are not drawn to the scale).

Table 1

Concentration of nitrites (NO₂⁻), nitrates (NO₃⁻) and hydrogen peroxide (H₂O₂), pH and ORP in PAW.

	NO ₂ ⁻ (mg/L)	NO ₃ ⁻ (mg/L)	H ₂ O ₂ (mg/L)	pH	ORP (mV)
Tap Water	ND	ND	ND	8.0 ± 0.1	-45.3 ± 2.4
PAW	32.4 ± 5.5	462 ± 1	8.80 ± 0.36	2.3 ± 0.1	292.0 ± 10.2

Table 2

Sample codes with corresponding compositions of the chemicals and solvents used throughout the study (SA-sodium alginate, g-glycerol, CA-citric acid, P/PAW-Plasma Activated Water, DW-Deionized water).

Sample Code	SA % (w/v)	g % (w/v)	CA % (w/v)	SHP % (w/v)	Solvent	pH
SA	2	0	0	0.0	DW	5.6
SA-gly	2	0.30	0	0.0	DW	5.6
SA-0.5CA	2	0	0.50	0.25	DW	3.6
SA-1.0CA	2	0	1.00	0.50	DW	3.0
SA-2.0CA	2	0	2.00	1.00	DW	2.8
SA-gly-0.50CA	2	0.30	0.50	0.25	DW	3.6
SA-gly-1.0CA	2	0.30	1.00	0.50	DW	3.0
SA-gly-2.0CA	2	0.30	2.00	1.00	DW	2.8
SA-P	2	0	0	0.0	PAW	2.5
SA-gly-P	2	0.30	0	0.0	PAW	2.6
SA-P-1.0CA	2	0	1.00	0.50	PAW	2.4
SA-gly-P-1.0CA	2	0.30	1.00	0.50	PAW	2.4

2.5. Mechanical properties

Tensile strength (TS), tensile modulus (TM) and Elongation at Break (EB) of the SA films were measured using a TA.XT plus texture analyser (Stable Micro Systems Ltd, Godalming, UK), equipped with a 500 kg load cell, with a crosshead speed of 1 mm/s and at a span distance of 25 mm, following the ASTM D638-699 method (1999). The dimensions of the films used for the test were 60 mm × 15 mm × 0.02 mm (length x width x thickness) as recommended by the standard ISO 14125. Films thickness was measured with a Japan Mitutoyo 500-197-20/30 200 mm/ 8'' Digital Digimatic Vernier Caliper (0.01 mm resolution; ± 0.02 mm accuracy). Triplicates of each sample were performed and analysed using the software Exponent ver: 6.1.16.0.

2.6. Rheological properties

Rheological properties were determined using a hybrid rheometer

(Discovery HR-2, TA Instruments, Newcastle, UK) and a cone and plate geometry (40 mm, 2°) at 22 °C. Approximately 1 mL of the sample was loaded onto the cross-hatched Peltier plate and subjected to frequency and amplitude sweeps over the range of 0.1–150 rad/s and 0.01–1000 % (points per decade 5) at the constant strain and frequency of 1.0 % and 1.0 rad/s, respectively. The strain limit (%) of the viscoelastic region (LVE) of the sample was determined by using the package “Segmented” (Muggeo, 2008) in the R program (The R Foundation for Statistical Computing, Vienna). Flow properties of the sample were determined over a shear rate range of 0.01–1000 s⁻¹ (points for decade 5) with the maximum equilibration time of 60 s using Steady state sensing function in TRIOS software (TA Instruments, version 4.3).

2.7. Water vapour transmission rate

The water vapour transmission rate (WVTR) of the films was measured according to the monograph of the European Pharmacopoeia (Sarwar, Niazi, Jahan, Ahmad, & Hussain, 2018). To determine moisture permeability, the SA films were cut into 15 mm diameter discs and then mounted on a cylindrical bottle with 13 mm diameter containing 10 mL of DW water followed by sealing with parafilm. The bottle was then kept in an oven at 45 °C for 24 h. The WVTR was calculated using the following equation:

$$WVTR = \frac{(w_i - w_f)}{A \times 24} \times 10^6 \text{ g m}^{-2}\text{h}^{-1}$$

where, A is the area of the bottle mount (m²), w_i and w_f are the weight of the bottle at time zero and the weight of the bottle after 24 h.

2.8. Statistical analysis

Average values and standard deviation were computed, and statistical analysis was performed using the Prism software package (version 3.02, GraphPad Software, San Diego, CA, USA, <http://www.graphpad.com>). Two-way analysis of variance (ANOVA) was performed with the bonferroni post-test to compare the significance of change in one factor with time. The error bars presented represent standard deviation with n = 3.

3. Results and discussion

3.1. Alginate with citric acid

Fig. 2[A] and [B] represent the effect of glycerol and/or citric acid (0.5, 1.0 and 2.0 % w/v) on the tensile strength (TS) & tensile modulus (TM) and elongation at break (EB) of SA films, respectively. The TS and

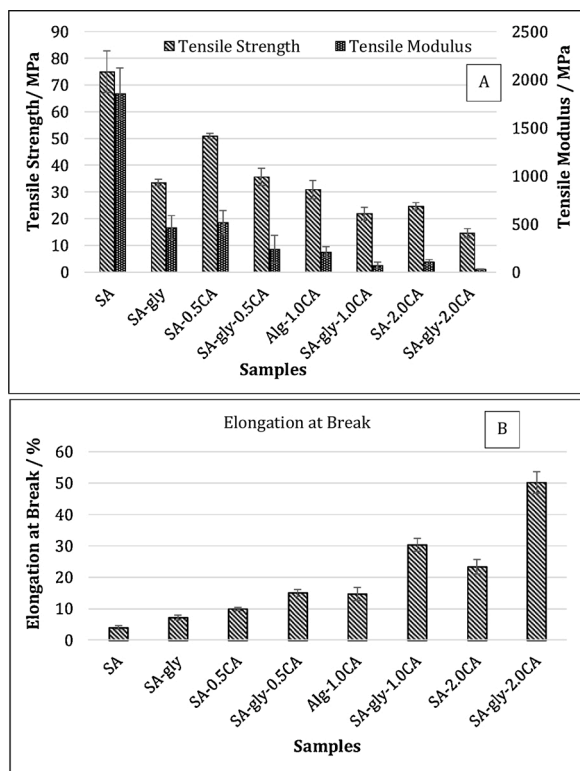


Fig. 2. Tensile Strength & Tensile Modulus [A] and Elongation at Break [B] of Sodium Alginate 2% w/v (SA), with glycerin (SA-gly) and with 0.5 % w/v [0.5 CA], 1% w/v [1.0 CA] and 2% w/v [2.0 CA] citric acid (CA).

TM were reduced by 55 % and 75 %, respectively, as 30 % w/w of glycerol (SA-gly) was added to 2% SA films. Addition of CA also reduced the TS and TM of SA films. However, the TS values for films with 0.5, 1.0 and 2.0 % CA containing SA films were significantly higher than the films containing glycerin with similar amount of CA. Moreover, at 0.5 % CA addition, the TS decreased by 32 % as compared to SA films, which was still 35 % higher than SA-g films. With further addition of 1.0 and 2.0 % of CA, the TS reduced by 58 % and 66 % as compared to the control SA films. No significant difference was observed between the TS values between the SA-g and SA-gly-0.5CA films. The lowest TS (15 MPa) was observed for SA-gly-2.0CA films. On the other hand, no statistically significant difference was observed between the TM values of SA-gly & SA-0.5CA, SA-0.5CA & SA-1.0CA and SA-gly-1.0CA & SA-gly-2.0CA films. With regards to the EB, the lowest value (4%) was observed for control SA films, which significantly increased with glycerin addition (7%). Likewise, increasing concentrations of CA also caused a significant increase in the EB values, reaching 10, 15 and 23 % in 0.5, 1.0 and 2.0 % CA containing films, respectively. Moreover, a synergistic effect, more pronounced with increasing CA levels, was observed when glycerol was combined with CA, achieving EB values of 15, 30 and 50 % for 0.5, 1.0 and 2.0 % CA containing SA films, respectively.

It is well known that the addition of low molecular weight plasticizers such as glycerol with high molecular mobility, can act as filler in the solvent-rich phase of the films, making them effective in disrupting the hydrogen bonds between polymer chains (Pongjanyakul, 2007). Such a disruption can increase the free volume, which may allow increased movement between the polymer chains, resulting in reduced TS and increased EB (Vieira, da Silva, dos Santos, & Beppu, 2011). Therefore, the reduction in TS and improvement in EB with glycerol addition could be attributed to the reduction in inter- and intra-molecular hydrogen bonding in the alginate network. Wu et al. studied the effect of citric acid cross-linking on the mechanical properties of corn starch-chitosan composite films (Wu et al., 2019). The

addition of up to 15 % CA was reported to increase the TS as compared to control samples, due to the inter and intra-molecular cross-linking between polymer chains by CA. However, with further addition of CA up to 20 % the TS reduced while the EB increased, which is similar to the results observed in the present study. Moreover, the reduction in the TS at higher CA content was attributed to the presence of unreacted CA, which may serve as a plasticizer (Wu et al., 2019). Therefore, CA may act as both cross-linking agent and plasticizer in the biopolymer films, especially at high concentration. Similar plasticizing effect of high CA concentration on the mechanical properties of biopolymer composite films was also reported by Want et al. and Reddy et al. (Reddy & Yang, 2010; Wang, Ren, Li, Sun, & Liu, 2014). Therefore, it could be concluded that when CA is added to a polymer structure, depending on the amount, there may exist some unreacted CA which may act as a plasticizer and can reduce the interactions between macromolecules resulting in reduced TS and increased EB values.

Fig. 3(A) and (B) represent the amplitude sweep curves for SA samples without and with glycerol, respectively. The corresponding strain values for the samples extracted from the amplitude sweep curves are presented in Table 3. The linear viscoelastic (LVE) region for SA films was located at a strain value of 39 %, which reduced to 25 %, 16 % and 10 % for 0.5 (SA-0.5CA), 1.0 (SA-1.0CA) and 2.0 % CA (SA-2.0CA), respectively. In general, the glycerol containing samples showed a shorter LVE region and lower limit strain of the LVR as compared to samples without glycerol. The shortest LVE region (lowest limit strain of the LVR) was observed for 2.0 % CA containing samples with glycerol (SA-gly-2.0CA), where the LVE region reduced to a strain of about 4%. The strain values obtained from the amplitude sweeps in this study correlates well with the tensile strength data (Fig. 1), indicating the plasticizing effect of unreacted CA present in the gel structure.

The storage modulus (G') of SA samples without or with glycerol are shown in Fig. 5(A) and (B), respectively. Overall, the G' at all

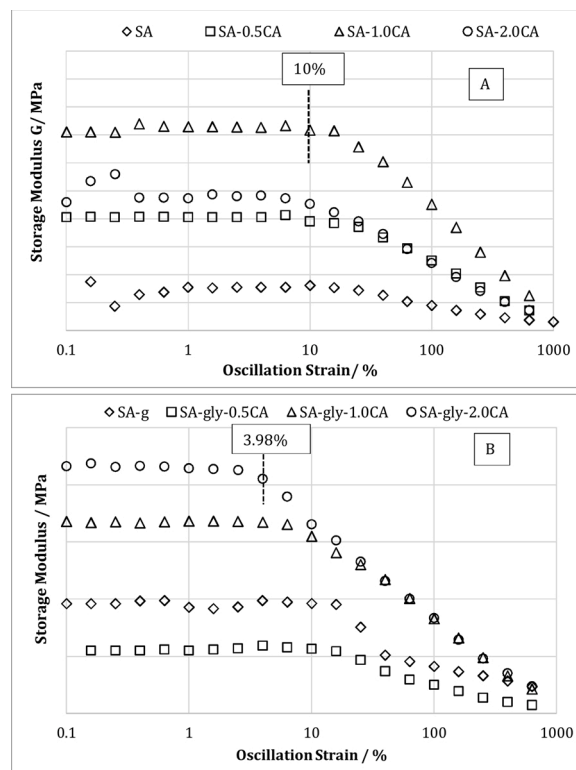


Fig. 3. Oscillatory amplitude sweep of Sodium Alginate (SA) [A] and SA containing glycerin (gly) and with 0.50 % [0.5CA], 1.0 % [1.0 CA] and 2% w/v [2.0CA] citric acid (CA) [B]. The Level strain % for SA-1.0CA and SA-gly-2.0CA is marked in figure (A) and (B), respectively.

Table 3

Limit strain of the LVE % of SA films containing or not glycerin and with 25, 50 and 100 % (w/w) citric acid (CA), acquired from corresponding oscillatory amplitude sweeps.

Samples	Strain %	Samples	Strain %
Alg	39.8196	SA-g	15.8521
SA-25CA	25.119	SA-g-25CA	15.0086
SA-50CA	15.84	SA-g-50CA	6.31
SA-100CA	10.00	SA-g-100CA	3.98

frequencies of 1.0 and 2.0 % CA containing samples was higher than the respective values for the control SA samples. For 0.5 % CA containing samples, the G' at lower frequencies was higher than the values for SA samples. However, at high frequencies, both SA and 0.5 % CA containing samples showed similar G' values. The increase in the G' often refers to an increase of the deformation energy required for the destruction of the internal gel structure, which has been attributed to the cross-linking between alginate chains via CA (Hilbig, Hartlieb, Gibis, Herrmann, & Weiss, 2020). A possible cross-linking reaction between alginate chains via CA is presented in Fig. 4. Fig. 6(A) shows the relationship between the storage (G') and loss modulus (G'') for control SA samples. The G'' of SA samples was higher than the G' at low frequencies and vice versa at higher frequencies, which is a typical behavior of non-cross linked polymer samples (Hilbig et al., 2020). Fig. 6(B) represents the relationship between the G' and G'' of SA samples containing 2.0 % CA. No intersection between G' and G'' was observed, regardless of the frequency, and the G'' of the samples was lower than the G' at all frequencies, which confirms the cross-linking of SA chains with CA. The 0.5 and 1.0 % CA containing samples showed a similar trend with regards to the G' and G'' , with no intersection observed between them (Figure not shown). Therefore, with CA addition, the elastic properties exceeded the

viscous properties, irrespective of the frequency indicating the cross-linking of the alginate gel by CA. Moreover, it should be noted that the pH values of the CA containing samples were well below 5 (see Table 2) and at low pH values stronger hydrogen bonds may have been formed, as the enhanced protonation of the acid residues reduces the electrostatic interactions between polymers chains (Gawkowska, Cybulska, & Zdunek, 2018). Therefore, the observed result could be attributed to the acidic cross-linking of alginate gels.

The relationship between the viscosity and shear rate of the SA + CA systems without and with glycerol is presented in Fig. 7(A) and (B), respectively. The CA containing solutions showed shear thinning or non-Newtonian properties, and thus the viscosity decreased with increasing shear rate, whereas this behaviour was not observed in the control SA samples, irrespective of the glycerol addition. Such a decrease in the viscosity with increasing shear rate has been attributed to the destruction of the SA molecular structure by shear stress, which can be explained by the disentanglement theory (Pamies, Schmidt, Martínez, & Torre, 2010). Addition of 0.5 % CA (pH = 3.6) did not cause any significant shift in the viscosity and shear dependence, as compared to the SA samples. For 0.5 % (pH = 3.2) and 2.0 % (pH = 2.8) CA containing samples, a significant increase in viscosity and shear dependence was observed. Addition of higher CA levels may enable more interchain interactions, resulting in more pronounced non-Newtonian behavior. A synergistic interaction between SA and CA was observed with regards to the increase in viscosity with increasing CA levels. Moreover, it has been reported that the viscosity of SA solutions is nearly constant between pH 6 and 7 (Yotsuyanagi, Yoshioka, Segi, & Ikeda, 1991). However, a decrease in pH to 3.5 could increase the viscosity, which is attributed to the formation of physical gels, where hydrogen bond attractions predominate over electrostatic repulsion (Gatej, Popa, & Rinaudo, 2005; Hassan & Abd-Alla, 2003; Saric, Schofield, & Keen, 1946; Yotsuyanagi

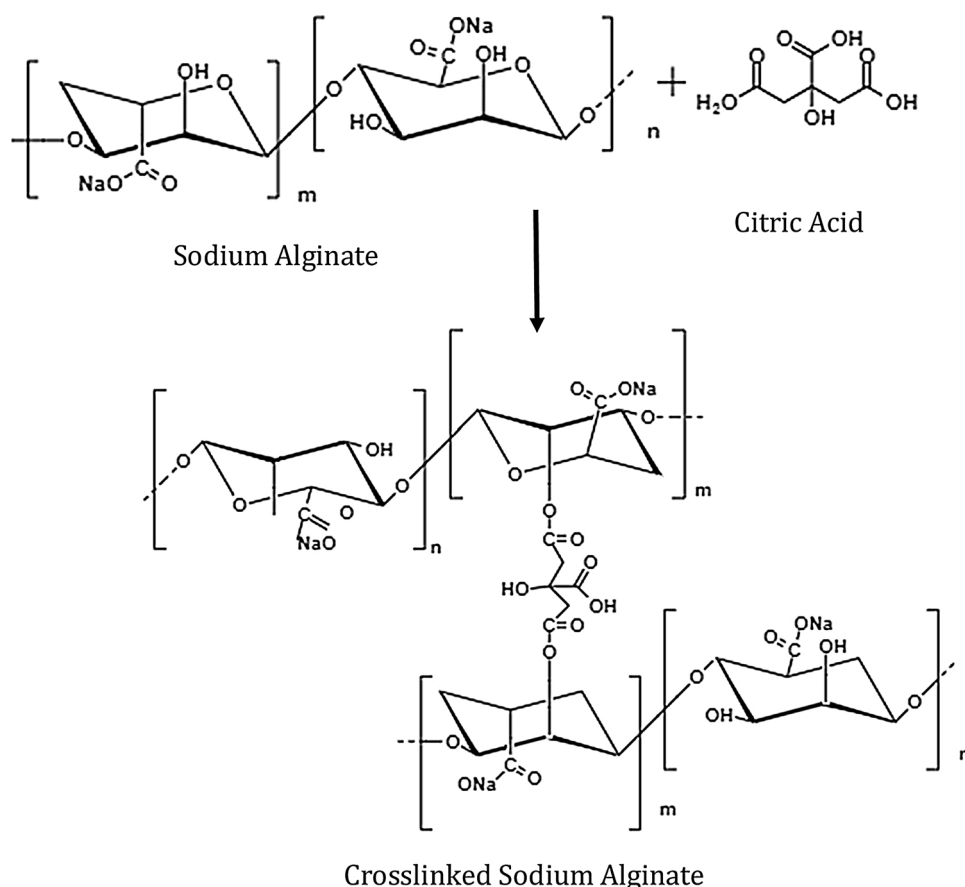


Fig. 4. Cross-linking reaction between sodium alginate chains by citric acid.

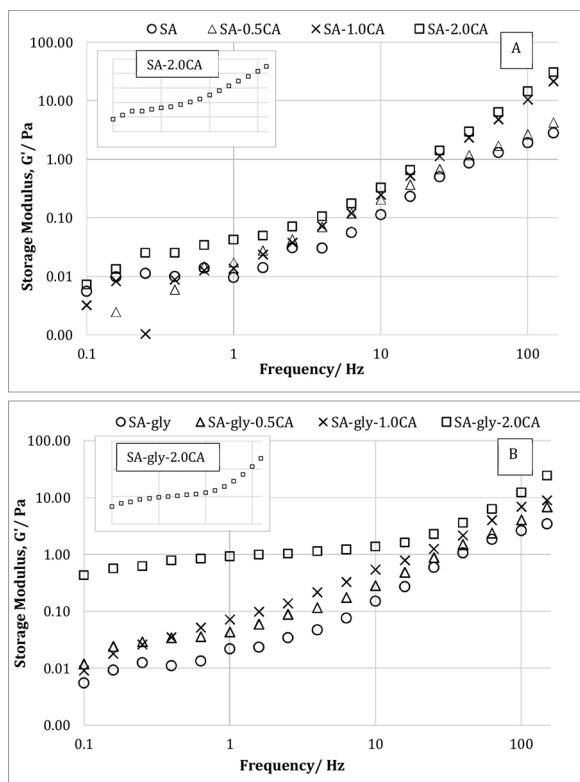


Fig. 5. Oscillatory frequency sweep of Sodium Alginate (SA) [A] and SA containing glycerin (g) [B] with 0.50 % [0.5CA], 1.0 % [1.0 CA] and 2% w/v [2.0CA] citric acid (CA). The inserted small figures for the oscillatory frequency sweep of SA-2.0CA (A) and SA-gly-2.0CA (B) has been added show the pattern without overlapping lines.

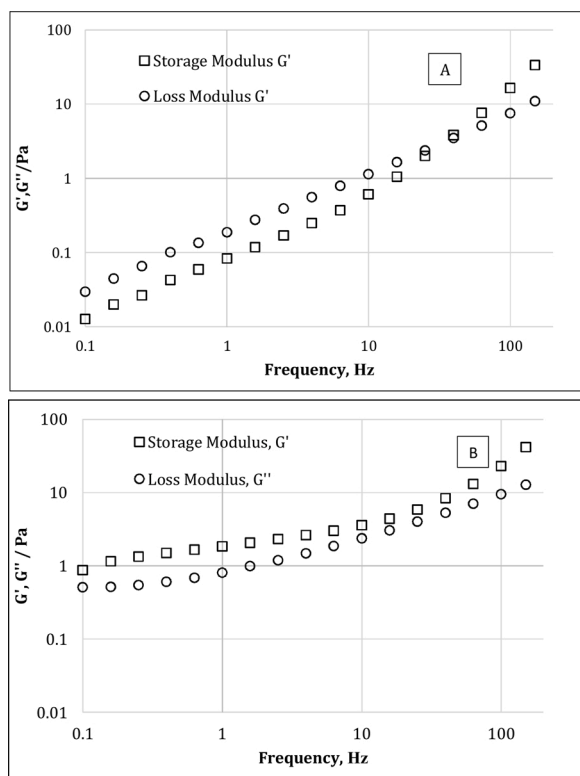


Fig. 6. Relationship between the storage modulus (G') and loss modulus (G'') of sodium alginate (SA) [A] and SA with 2% [SA-2.0CA] (w/v) citric acid (CA).

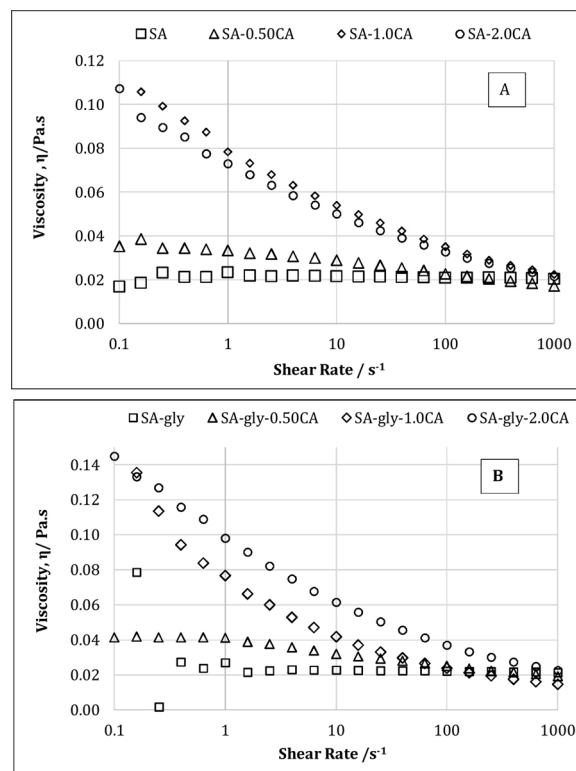


Fig. 7. Shear flow curves of Sodium Alginate (SA) [A] and SA containing glycerin [B] with 0.50 % [0.5CA], 1.0 % [1.0 CA] and 2% w/v [2.0CA] citric acid (CA).

et al., 1991).

The effect of glycerol and citric acid on the WVTR of SA films is presented in Fig. 8. The WVTR of SA film was $32 \text{ g}\cdot\text{mm}^{-2}\cdot\text{hr}^{-2}$, which increased to $36 \text{ g}\cdot\text{mm}^{-2}\cdot\text{hr}^{-2}$ with the addition of 30 % glycerol (SA-g). The WVTR rate reduced to $28 \text{ g}\cdot\text{mm}^{-2}\cdot\text{hr}^{-2}$ and $21 \text{ g}\cdot\text{mm}^{-2}\cdot\text{hr}^{-2}$ when 0.5 % (SA-0.5CA) and 1.0 % (SA-1.0CA) CA were added to the SA films. The reduction in the WVTR rate could be due to the decreased availability of hydrophilic hydroxyl groups and generated hydrophobic ester groups between citric acid and the polysaccharides (Fig. 4), resulting in a denser structure and thus, improved WVTR. However, with 2.0 % CA addition, the WVTR increased to $28 \text{ g}\cdot\text{mm}^{-2}\cdot\text{hr}^{-2}$. The increase in the WVTR could be due to the plasticizing effect of the excess or unreacted CA present with 2.0 % CA addition. Guibert and Biquet reported that the addition of plasticizers can increase the WVTR by reducing the intermolecular bonds between the polymer chains. Contrary to this, addition

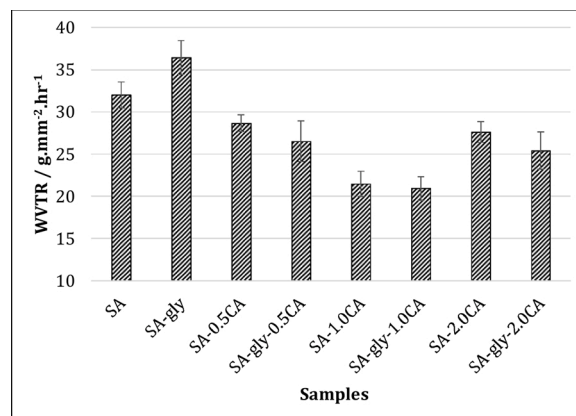


Fig. 8. Effect of glycerol (g) and citric acid (CA) on the Water vapour transmission rate (WVTR) of sodium alginate (SA) films.

of glycerol did not cause any significant difference in the WVRT of the CA containing SA films. Olivas et al. suggested that the presence of microstructure in the films without the plasticizers may be responsible for the high WVRT (Olivas & Barbosa-Cánovas, 2008). Based on the mechanical, rheological and WVTR of CA containing SA films, only 1.0 % CA containing solution was selected to evaluate the combined effect of CA and PAW on alginate cross-linking.

3.2. Combined effect of CA and PAW on alginate

The effect of PAW on the mechanical properties of SA films is shown in Fig. 9, as well as the results of its combination with 1.0 % CA, in the presence or absence of glycerol. The TS and TM for SA films prepared with PAW (SA-P) were 112 and 2240 MPa, respectively (Fig. 9A), about 33 % and 17 % higher than the values observed for the control SA films. The EB for SA-P films was 5.4 %, about 26 % higher than the corresponding value for the control SA films (Fig. 9B). With 30 % glycerol addition (SA-P-gly), the TS of SA-P films reduced by 44 %, while the EB increased by almost 50 %. A reduction of 22 % and 43 % in the TS was also observed when 1.0 % CA was added to SA-P films in presence and absence of glycerol, respectively. However, the TS values of SA-P-1.0CA and SA-P-gly-1.0CA films were still 41 and 48 % higher than the corresponding values in absence of CA. On the other hand, the EB of SA-P and SA-P-gly films increased by 66 and 71 %, respectively, with the

addition of PAW. Moreover, the addition of 1.0 % CA increased the EB values by 18 % and 14 % as compared to SA-P and SA-P-gly films, respectively. Therefore, it could be concluded that the films prepared with PAW showed better mechanical properties as compared to the ones made with deionized water.

Fig. 10 represents the amplitude sweep curves for SA-P samples containing 1.0 % CA. The corresponding level strain values for the samples extracted from the amplitude sweep curves are presented in Table 4. It is well known that in the LVE region, the G' is independent of the strain (Liu, Qian, Shu, & Tong, 2003). For PAW-based SA samples, the LVE region was observed over the strain range of 10–63%, the latter value being 38 % higher than that for the control SA samples. When 1.0 % CA was added to SA-P samples (SA-P-1.0CA), the maximum strain value for the LVE region was reduced to 25 %. Moreover, a further reduction in the LVE region was observed with glycerol addition. However, the samples prepared with PAW showed longer LVE region as compared to the samples prepared with deionized water.

In general, the interaction between CP and water results in a combination of reactive oxygen and nitrogen species (RONS), which have been reported to dissolve and react with water molecules, forming a cocktail of chemical species, with high oxidations redox potential and low pH. For instance, nitrogen oxides (NOx) are formed in air plasma through gas-phase reactions of dissociated N_2 and O_2 , which dissolve in water forming nitrites and nitrates. The concentrations of nitrites and nitrates in the PAW are listed in Table 1. Nitrites and nitrates in PAW can cause cross-linking between alginate chains and thus, improve the mechanical properties. A possible cross-linking reaction between alginate chains by nitrates is given in Fig. 9[C]. Moreover, it is also possible that the excess of CA cross-linked with each other or with glycerol in presence of RONS. Such cross-linking reactions can reduce the excess of or unreacted CA present in the gel structure and thereby, its plasticizing effect, thus improving the mechanical properties. Similar cross-linking reaction between CA and glycerol was reported by Halpern et al. (2014). Moreover, it should also be noted that the dissolution of NOx in water can produce H^+ ions which can cause the pH to drop. Moreover, hydrogen peroxide is also formed, which also reduces the pH. In the present study, the pH of the PAW containing samples ranged between 2.4 and 2.5 (see Table 1).

As already mentioned, at a pH level below 5 the free carboxyl groups COO^- present in the alginate structure are protonated to $COOH$, which reduces the electrostatic interactions between the alginate chains, and as a result, the alginate chains are able to arrange more closely forming hydrogen bonds (Andriamanantoanina & Rinaudo, 2010b). Therefore, the protonation in acidic conditions can promote the hydrogen bond formation within alginate chains, thus being responsible for enhanced mechanical properties and extended LVE region. It has also been reported that the formation of such proton-induced intermolecular associations by shielding the negative charges of the alginate polymers, may also increase the viscosity and G' , as was observed in the present study (Figs. 11 and 13) (Marcos, Gou, Arnau, & Comaposada, 2016). Fig. 12 shows the dependency of the G' with the frequency for SA samples prepared with PAW. The G' of SA-P samples was higher than that of SA samples, which could be due to the cross-linking of the alginate network by the RONS in the PAW. A further increase in the G' was also observed as 1.0 % CA was added to SA-P solutions. The high G' of PAW + CA containing samples could be attributed to the dual cross-linking of the alginate structure by CA and the RONS present in the PAW. The variability of the G' and G'' of SA-P and SA-P-50CA samples with the frequency is shown in Fig. 13. The G' of the samples was higher than the G'' and no intersection was observed. Andriamanantoanina and Rinaudo studied the relationship between the molecular structure of alginates and their gelation in acidic conditions (Andriamanantoanina & Rinaudo, 2010a). They reported that at pH 3.05, the G' and G'' were almost similar. However, with further decrease in the pH, the G' became higher than G'' due to formation of a gel-like system with interacting chain segments. They concluded that the gel was induced at pH 3.0,

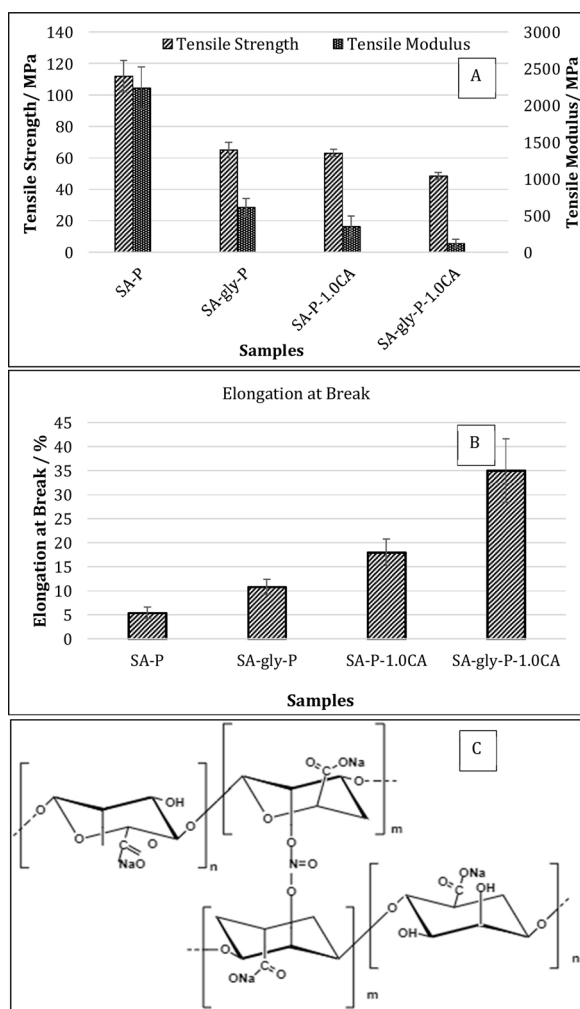


Fig. 9. Tensile strength & modulus [A] and elongation at break [B] of sodium alginate (SA) films prepared with PAW, with and without glycerol addition and/or with 1% w/v citric acid (CA); [C] a possible crosslinking reaction between alginate chains by nitrates from PAW.

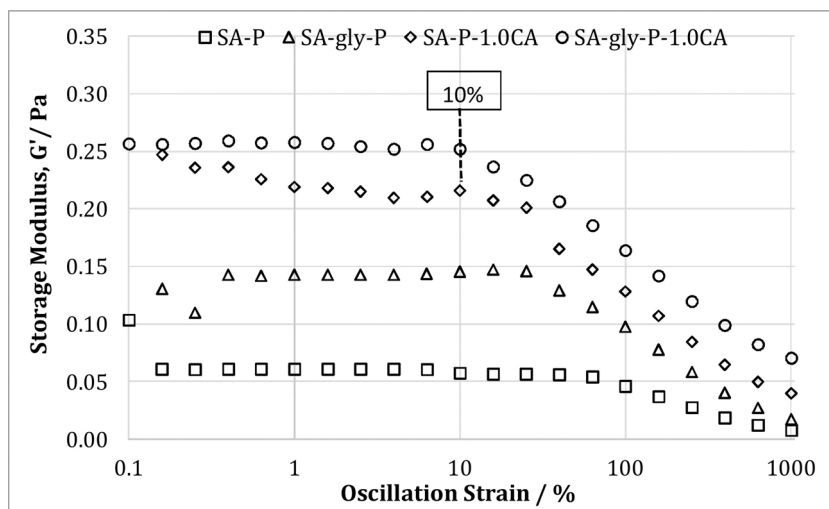


Fig. 10. Oscillatory amplitude sweep of Sodium Alginate (SA) and SA containing glycerin (g) with 1% w/v [1.0CA] citric acid (CA).

Table 4
Limit strain of the LVE % of Sodium Alginate (SA) and SA containing glycerin (g) with 50 % [CA(50)] (w/w) citric acid (CA).

Samples	Strain %
SA-P	63.1105
SA-g-P	25.1214
SA-P-50CA	25.1157
SA-g-P-50CA	10.0002

corresponding to the intrinsic pK of the carboxyl groups.

The variability of the viscosity of PAW containing samples with the shear rate is represented in Fig. 13. All the samples showed shear thinning or non-Newtonian behavior as the viscosity of the samples decreased with increasing shear rate. Moreover, the dependency of the viscosity with the shear rate increased with the CA addition. The addition of PAW caused a shear thinning effect, not observed in SA samples, thus confirming the cross-linking of alginate chains by RONS. Further increase in viscosity of SA-P samples with CA addition was attributed to the dual cross-linking of the alginate chains by CA and RONS. Pamies

et al. reported that shear thinning or non-Newtonian behavior is more pronounced for longer chains, due to increase in the extent of entanglement (Pamies et al., 2010). Therefore, a more significant shear thinning effect is expected as a result of dual PAW-CA crosslinking due to the presence of higher number of interpolymer interactions that can be disrupted by shear flow.

The effect of PAW on the WVTR of sodium alginate films is presented in Fig. 14. The WVTR rate of SA-P samples ($28 \text{ g}\cdot\text{mm}^{-2}\cdot\text{hr}^{-1}$) was significantly lower than that of SA films ($32 \text{ g}\cdot\text{mm}^{-2}\cdot\text{hr}^{-1}$), which could be due to the cross-linking of alginate chains by the RONS in the PAW. While the addition of glycerol increased WVTR of SA-g-P films to $33 \text{ g}\cdot\text{mm}^{-2}\cdot\text{hr}^{-1}$, 1.0 % CA (SA-P-50CA) reduced it to $18 \text{ g}\cdot\text{mm}^{-2}\cdot\text{hr}^{-1}$, which was significantly lower than the value for SA-1.0CA films (no PAW), and thus attributed to the double cross-linking of alginate chains by CA and RONS. No statistically significant differences in the WVTR values were observed between SA-P-1.0CA and SA-gly-P-1.0CA films.

4. Conclusions

In the present study, the effect of three different concentrations (0.5, 1 and 2% w/v) of citric acid on the mechanical, rheological and barrier

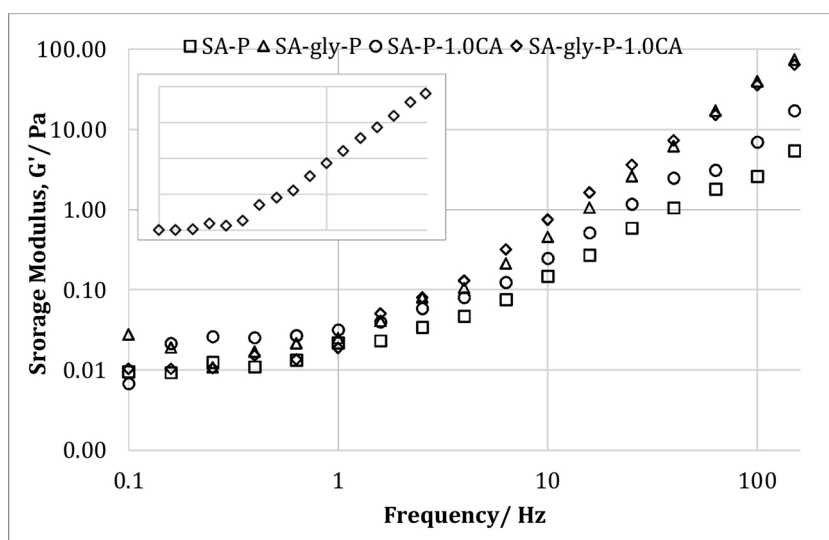


Fig. 11. Oscillatory frequency sweep of sodium alginate prepared with PAW (SA-P), containing glycerin (g) and with 1% w/v [1.0CA] citric acid (CA). The inserted small figure for the oscillatory frequency sweep of SA-gly-P-1.0CA has been added show the pattern without overlapping lines.

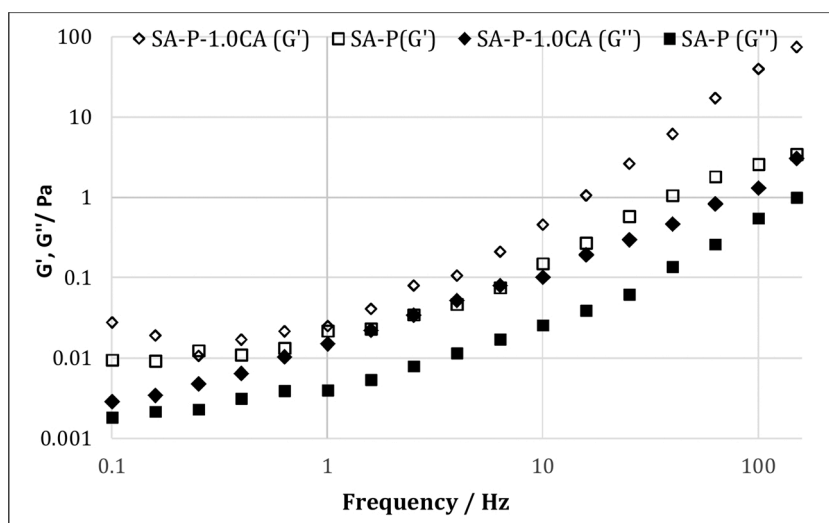


Fig. 12. Relationship between the storage modulus (G') and loss modulus (G'') sodium alginate solution prepared with PAW (SA-P) and with 1% w/v [1.0CA] citric acid (CA).

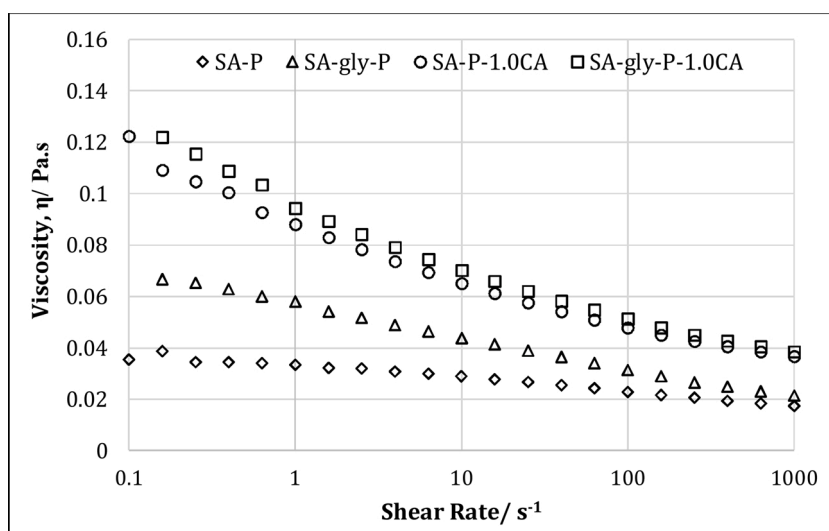


Fig. 13. Shear flow curves of sodium alginate prepared with PAW (SA-P), containing glycerin (g) and cross-linked with 1% w/v [1.0CA] citric acid (CA).

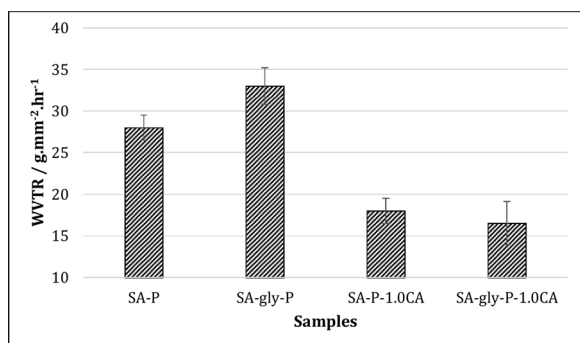


Fig. 14. Water vapour transmission rate (WVTR) of sodium alginate prepared with PAW (SA-P) and SA-P containing glycerin (g) with 1% w/v [1.0CA] citric acid (CA).

properties of sodium alginate solutions and films was evaluated. Moreover, the effect of plasma activate water alone and in combination with 1% w/v citric acid on the mechanical, rheological and barrier properties

of the alginate films were also studied. A decrease in the tensile strength and tensile modulus and a remarkable improvement in elongation at break of SA films was observed with both increasing CA content and glycerol addition. When PAW was used for the preparation of SA films, the tensile strength, tensile modulus, and elongation at break increased by 33, 17 and 26 %, respectively, as compared to the control SA films. When 1% CA was added, the tensile strength of the PAW-based SA films reduced by 43 %, while the elongation at break increased by 66 %, both parameters being, respectively, 41 % and 18 % higher than the respective values when deionized water was used instead.

From amplitude sweep data, the LVE decreased with the addition of glycerol and increasing CA content. From frequency sweep data, the G' was higher in 50 and 100 % CA containing samples than in the control SA samples, regardless of the frequency. However, the G' of 0.5 % CA containing samples was higher than the value for SA samples at lower frequencies, while at higher frequencies the respective values became similar. The LVE and the G' were remarkably higher for PAW-based samples, as compared to the equivalent ones prepared with deionized water. Moreover, the G'' of SA samples was higher than the G' at low frequencies and vice versa at higher frequencies, which is a typical behavior of non-cross-linked polymer samples. However, for CA

containing samples, the G'' was lower than the G' at all frequencies and no intersection was observed between them, which confirms the cross-linking of SA chains with CA. Similarly, no intersection between G' and G'' was observed for PAW-based samples. Both CA and PAW containing samples showed shear-thinning or non-Newtonian behaviour, which was not observed in SA samples, irrespective of glycerol addition. The WVTR decreased with the addition of 0.5 and 1% CA, although a further increase to 2% CA did not cause a significant difference in this parameter, as compared to 0.5 % CA. The WVTR of PAW containing samples was significantly lower than the values for the equivalent samples prepared with deionized water. In general, addition of glycerol to the samples resulted in reduced WVTR. The present study has demonstrated the effect of CA in combination with PAW and glycerol on the enhanced mechanical, rheological and barrier properties of the alginate films for potential food packaging applications.

Disclaimer

The author, Estefanía Noriega Fernández, is employed with the European Food Safety Authority (EFSA) at the Nutrition Unit that provides scientific and administrative support to the Panel on “Nutrition, Novel Foods and Food Allergens” in the area “Safety Assessment of Novel Foods”. However, the present article is published under the sole responsibility of the authors N. Sharmin, I. Sone, J. Walsh, M. Sivertsvik, E. Noriega Fernández and may not be considered as an EFSA scientific output. The positions and opinions presented in this article are those of the author/s alone and are not intended to represent the views/any official position or scientific works of EFSA. To know about the views or scientific outputs of EFSA, please consult its website under <http://efsa.europa.eu>.

Declaration of Competing Interest

The authors report no declarations of interest.

Acknowledgement

The authors would like to thank Nofima Strategic Programme “PackTech” for funding the work.

References

- Andriamanantoanina, H., & Rinaudo, M. (2010a). Relationship between the molecular structure of alginates and their gelation in acidic conditions. *Polymer International*, 59(11), 1531–1541.
- Andriamanantoanina, H., & Rinaudo, M. (2010b). Relationship between the molecular structure of alginates and their gelation in acidic conditions. *Polymer International*, 59, 1531–1541.
- Azeredo, H. M. C., & Waldron, K. W. (2016). Crosslinking in polysaccharide and protein films and coatings for food contact – A review. *Trends in Food Science & Technology*, 52, 109–122.
- Carissimi, M., Flores, S. H., & Rech, R. (2018). Effect of microalgae addition on active biodegradable starch film. *Algal Research*, 32, 201–209.
- Cazón, P., Velazquez, G., Ramírez, J. A., & Vázquez, M. (2017). Polysaccharide-based films and coatings for food packaging: A review. *Food Hydrocolloids*, 68, 136–148.
- Eisenberg, G. (1943). Colorimetric determination of hydrogen peroxide. *Industrial & Engineering Chemistry Analytical Edition*, 15(5), 327–328.
- Fan, H. Y., Duquette, D., Dumont, M.-J., & Simpson, B. K. (2018). Salmon skin gelatin-core zinc composite films produced via crosslinking with glutaraldehyde: Optimization using response surface methodology and characterization. *International Journal of Biological Macromolecules*, 120, 263–273.
- Gao, C., Pollet, E., & Avérous, L. (2017). Properties of glycerol-plasticized alginate films obtained by thermo-mechanical mixing. *Food Hydrocolloids*, 63, 414–420.
- Gatej, I., Popa, M., & Rinaudo, M. (2005). Role of the pH on hyaluronan behavior in aqueous solution. *Biomacromolecules*, 6(1), 61–67.
- Gawkowska, D., Cybulska, J., & Zdunek, A. (2018). Structure-related gelling of pectins and linking with other natural compounds: A review. *Polymers*, 10(7), 762.
- Griess, P. (1879). Bemerkungen zu der Abhandlung der HH. Weselsky und Benedikt “Ueber einige Azoverbindungen”. *Berichte der deutschen chemischen Gesellschaft*, 12 (1), 426–428.
- Halpern, J. M., Urbanski, R., Weinstock, A. K., Iwig, D. F., Mathers, R. T., & von Recum, H. A. (2014). A biodegradable thermoset polymer made by esterification of citric acid and glycerol. *Journal of Biomedical Materials Research Part A*, 102(5), 1467–1477.
- Hassan, R., & Abd-Alla, M. (2003). Ionotropic gels of alginate polyelectrolyte. I. Potentiometric determination of the ionization constant of alginate acid polyelectrolyte in relation to sol-gel transformation mechanism. *Acta Polymerica*, 42, 447–450.
- Hilbig, J., Hartlieb, K., Gibis, M., Herrmann, K., & Weiss, J. (2020). Rheological and mechanical properties of alginate gels and films containing different chelators. *Food Hydrocolloids*, 101, 105487.
- Hua, S., Ma, H., Li, X., Yang, H., & Wang, A. (2010). pH-sensitive sodium alginate/poly(vinyl alcohol) hydrogel beads prepared by combined Ca²⁺ crosslinking and freeze-thawing cycles for controlled release of diclofenac sodium. *International Journal of Biological Macromolecules*, 46(5), 517–523.
- Khan, B., Niazi, M., Jahan, Z., Farooq, W., Raza Naqvi, S., Ali, M., et al. (2018). Effect of ultra-violet cross-linking on the properties of boric acid and glycerol co-plasticized thermoplastic starch films. *Food Packaging and Shelf Life*, 19.
- Kleinbongard, P., Rassaf, T., Dejam, A., Kerber, S., & Kelm, M. (2002). Griess method for nitrite measurement of aqueous and protein-containing samples. *Methods in Enzymology* (pp. 158–168). Academic Press.
- Lee, K., & Mooney, D. (2012). Alginate: Properties and biomedical applications. *Progress in Polymer Science*, 37, 106–126.
- Liu, X., Qian, L., Shu, T., & Tong, Z. (2003). Rheology characterization of sol-gel transition in aqueous alginate solutions induced by calcium cations through in situ release. *Polymer*, 44(2), 407–412.
- Marcos, B., Gou, P., Arnau, J., & Comaposada, J. (2016). Influence of processing conditions on the properties of alginate solutions and wet edible calcium alginate coatings. *LWT – Food Science and Technology*, 74.
- Muggeo, V. M. R. (2008). An R package to fit regression models with broken-line relationships. *R News*, (8), 20–25.
- Nasrollahzadeh, M., Sajjadi, M., Irvani, S., & Varma, R. S. (2021). Starch, cellulose, pectin, gum, alginate, chitin and chitosan derived (nano)materials for sustainable water treatment: A review. *Carbohydrate Polymers*, 251, 116986.
- Nilsen-Nygaard, J., Fernández, E. N., Radusin, T., Rotabakk, B. T., Sarfraz, J., Sharmin, N., et al. (2021). Current status of biobased and biodegradable food packaging materials: Impact on food quality and effect of innovative processing technologies. *Comprehensive Reviews on Food Science and Food Safety*, 20(2), 1333–1380.
- Oh, Y. A., Roh, S. H., & Min, S. C. (2016). Cold plasma treatments for improvement of the applicability of defatted soybean meal-based edible film in food packaging. *Food Hydrocolloids*, 58, 150–159.
- Olivas, G. I., & Barbosa-Cánovas, G. V. (2008). Alginate-calcium films: Water vapor permeability and mechanical properties as affected by plasticizer and relative humidity. *LWT – Food Science and Technology*, 41(2), 359–366.
- Olsson, E., Hedenqvist, M. S., Johansson, C., & Järnström, L. (2013). Influence of citric acid and curing on moisture sorption, diffusion and permeability of starch films. *Carbohydrate Polymers*, 94(2), 765–772.
- Pamies, R., Schmidt, R. R., Martínez, M. d. C. L., & Torre, J. G. d. l. (2010). The influence of mono and divalent cations on dilute and non-dilute aqueous solutions of sodium alginates. *Carbohydrate Polymers*, 80(1), 248–253.
- Pankaj, S., Bueno-Ferrer, C., Misra, N. N., Milosavljevic, V., O'Donnell, C., Bourke, P., et al. (2014). Applications of cold plasma technology in food packaging. *Trends in Food Science & Technology*, 35, 5–17.
- Pongjanyakul, T. (2007). Alginate-magnesium aluminum silicate films: Effect of plasticizers on film properties, drug permeation and drug release from coated tablets. *International Journal of Pharmaceutics*, 333, 34–44.
- Puscaselu, R., Gutt, G., & Amariei, S. (2019). Rethinking the future of food packaging: Biobased edible films for powdered food and drinks. *Molecules (Basel, Switzerland)*, 24(17), 3136.
- Qin, Z., Mo, L., Liao, M., He, H., & Sun, J. (2019). Preparation and characterization of soy protein isolate-based nanocomposite films with cellulose nanofibers and nano-silica via silane grafting. *Polymers*, 11(11), 1835.
- Reddy, N., & Yang, Y. (2010). Citric acid cross-linking of starch films. *Food Chemistry*, 118(3), 702–711.
- Risa Vaka, M., Sone, I., García Álvarez, R., Walsh, J. L., Prabhu, L., Sivertsvik, M., et al. (2019). Towards the next-generation disinfectant: Composition, storability and preservation potential of plasma activated water on baby Spinach leaves. *Foods*, 8 (12), 692.
- Russo, R., Malinconico, M., & Santagata, G. (2007). Effect of cross-linking with calcium ions on the physical properties of alginate films. *Biomacromolecules*, 8(10), 3193–3197.
- Saric, S. P., Schofield, R. K., & Keen, B. A. (1946). The dissociation constants of the carboxyl and hydroxyl groups in some insoluble and sol-forming polysaccharides. *Proceedings of the Royal Society of London Series A, Mathematical and Physical Sciences*, 185(1003), 431–447.
- Sarwar, M. S., Niazi, M. B. K., Jahan, Z., Ahmad, T., & Hussain, A. (2018). Preparation and characterization of PVA/nanocellulose/Ag nanocomposite films for antimicrobial food packaging. *Carbohydrate Polymers*, 184, 453–464.
- Shahabi-Ghahfarokhi, I., Almasi, H., & Babaei-Ghazvini, A. (2020). Characteristics of biopolymers from natural resources. In Y. Zhang (Ed.), *Processing and development of polysaccharide-based biopolymers for packaging applications* (pp. 49–95). Amsterdam, Netherlands: Elsevier.
- Tavassoli-Kafrani, E., Shekarchizadeh, H., & Masoudpour-Behabadi, M. (2016). Development of edible films and coatings from alginates and carrageenans. *Carbohydrate Polymers*, 137, 360–374.

- Thirumdas, R., Kothakota, A., Annapure, U., Siliveru, K., Blundell, R., Gatt, R., et al. (2018). Plasma activated water (PAW): Chemistry, physico-chemical properties, applications in food and agriculture. *Trends in Food Science & Technology*, 77, 21–31.
- Vieira, M. G. A., da Silva, M. A., dos Santos, L. O., & Beppu, M. M. (2011). Natural-based plasticizers and biopolymer films: A review. *European Polymer Journal*, 47(3), 254–263.
- Wang, S., Ren, J., Li, W., Sun, R., & Liu, S. (2014). Properties of polyvinyl alcohol/xylan composite films with citric acid. *Carbohydrate Polymers*, 103, 94–99.
- Wu, H., Lei, Y., Lu, J., Zhu, R., Xiao, D., Jiao, C., et al. (2019). Effect of citric acid induced crosslinking on the structure and properties of potato starch/chitosan composite films. *Food Hydrocolloids*, 97, 105208.
- Yotsuyanagi, T., Yoshioka, I., Segi, N., & Ikeda, K. (1991). Acid-induced and calcium-induced gelation of alginic acid: Bead formation and pH-dependent swelling. *Chemical & Pharmaceutical Bulletin*, 39(4), 1072–1074.
- Zou, Z., Zhang, B., Nie, X., Cheng, Y., Hu, Z., Liao, M., et al. (2020). A sodium alginate-based sustained-release IPN hydrogel and its applications. *RSC Advances*, 10(65), 39722–39730.